Effects of substrate heat accumulation on the cold sprayed Ni coating quality: Microstructure evolution and tribological performance

Chaoyue Chen, Yingchun Xie, Xinliang Xie, Xingchen Yan, Renzhong Huang, Jiang Wang, Zhongming Ren, Sihao Deng, Hanlin Liao

Version of Record: https://www.sciencedirect.com/science/article/pii/S0257897219304670
Manuscript_92f0747c09b437e7604120fb02717907

Effects of substrate heat accumulation on the cold sprayed Ni coating quality: microstructure evolution and tribological performance

Chaoyue CHEN[1, 3, 4#], Yingchun XIE[1, 2#*], Xinliang XIE[1], Xingchen YAN[1, 2], Renzhong HUANG[2], Jiang WANG[3], Zhongming REN[3], Sihao DENG[1], Hanlin LIAO[1, 4]

1. *ICB UMR 6303, CNRS, Univ. Bourgogne Franche-Comté, UTBM, F-90010 Belfort, France*
2. *National Engineering Laboratory for Modern Materials Surface Engineering Technology; The Key Lab of Guangdong for Modern Surface Engineering Technology; Guangdong Institute of New Materials, Guangzhou 510651, P.R. China*
3. *State Key Laboratory of Advanced Special Steels, School of Materials Science and Engineering, Shanghai University, Shanghai 200444, China*
4. *Sino-European School of Technology of Shanghai University, Shanghai 200444, PR China*

Abstract: The residual stress and distortion caused by non-uniform temperature distribution has limited the application of cold spray (CS) technique as an effective additive manufacturing and damage repair method for large-scale components. In order to investigate the influence of heat accumulation on coating quality, two types of CS Ni coatings with different building dimensions were deposited onto substrates. The type II Ni coatings with smaller fabrication size possess a fully dense microstructure without cracks, while the type I coatings with larger size show a significantly higher porosity value. The type II coatings show relatively higher microhardness. The tribological tests show that the type II Ni coatings present a better wear resistance with lower coefficient of friction and lower wear rate. The distinct worn morphologies show that the lower microhardness and porous microstructure of type I coatings lead to numerous delamination and exposure of interior coating. According to the temperature history recorded by infrared imaging camera, higher average temperature was found at the type II coatings due to enhanced heat accumulation of coating/substrate system at the short nozzle movement. The increased particle plastic deformation can further promote the coating densification rate and further ameliorate the coating quality. It can be summarized that the nozzle trajectory and deposition strategy can affect the temperature distribution and determine the coating qualities. This work provides a potential guidance for the optimization of coating quality by cold spraying additive manufacturing.

Keywords: cold spray; Ni coating; tribological test; heat accumulation; microstructure

#These authors contributed equally to this work;
*Corresponding author: Yingchun XIE (yingchun.xie@hotmail.com)

1. Introduction

Different from conventional subtractive manufacturing, the additive manufacturing (AM) is a technology that enables the direct fabrication of component with complex geometry [1, 2]. Based on the principle of CAD design, the AM techniques can effectively avoid extra material waste, realize personalized and customized fabrication, and shorten the production period. For the moment, various AM methods have been proposed and applied in industrial manufacturing, such as selective laser melting (SLM) [3, 4], electron beam melting (EBM) [5] and direct metal deposition (DMD) [6], etc. In these methods, the high-energy sources such as laser or electron beam are used to selectively melt the powder bed followed by rapid solidification. Then, the part can be built through the rapid melting and solidification layer-by-layer [1]. However, the production rate and fabrication size are restricted in the abovementioned AM methods.

Recently, the emerging cold spray (CS) technology has attracted increasing attention due to the distinct solid-state deposition well below the material melting point [7, 8]. In this CS deposition process, feedstock particles are accelerated to a high velocity (300 to 1200 m/s) through a de-Laval nozzle by the high-pressure propelling gas with low temperature (such as air, nitrogen or helium). Thus, the slightly heated particles are well maintained in solid-state. Based on the high-velocity impact on substrate, the particle can experience severe plastic deformation, and the successful coating deposition can be achieved as a result of combining metallurgical bonding [9] and mechanical interlocking [10]. Different from traditional thermal spray technologies, CS technique can extensively retain the original properties of feedstock, produce thick and dense coating with high deposition efficiency and avoid the oxidation as well as phase change. Compared with the laser or electron beam-based AM methods, CS technique demonstrates a significantly higher production rate without limitation in fabrication size. Recently, CS has been widely applied as an effective additive manufacturing technology for the production of large-scale bulk [11, 12], damage restoration [13] and topology optimization [14].

The understanding of the bonding mechanism is essential for further development of CS technology. Over the past few decades, principles of the bonding mechanism have been studied by experimental and numerical methods. Currently, mechanical interlocking and metallurgical bonding are considered as the main bonding mechanisms during the formation of cold sprayed coating [15, 16]. The most prevailing hypothesis speculates the important role of adiabatic shear instability (ASI) during the deposition process at

the particle/substrate interface. As the high strain rate and the intensive localized deformation during the particle deposition process, adiabatic shear instability (ASI) was occurred at the particle interface [15, 17]. Under the effects of ASI induced temperature arise, both the particle and substrate behave like a viscous material, which results in the metal jet at the rim of deformed area. It can disrupt thin oxide films on the surface of the material [18, 19]. The resulting oxide-free surface can provide an intimate contact between the particles and the substrate, then metallurgical bonding occurs at particle/substrate interface under high local pressure [15, 20-22]. According to current understanding of bonding mechanism, the properties of substrate and feedstock particles play crucial roles during the deposition of cold sprayed coating [23]. Related studies showed that the preheating of the substrate [24, 25] or feedstock particles [23, 26] can effectively improve the coating quality by ameliorating inter-particle cohesive bonding and promoting the adhesion bonding between coating/substrate. The thermal softening of the substrate can induce its severe plastic deformation under successive particle impact and resultant stronger particle interlocking [24, 25]. Meanwhile, the plastic deformation can also promote the breaking and cleaning of original oxide-film and further improve the metallurgical bonding at oxide-free interface [19]. Similarly, the particle preheating was also widely applied to reduce the critical deposition velocity of the particle [26, 27]. The metallurgical bonding within as-sprayed coating can also be improved as a result of a stronger plastic deformation.

However, the influence of dynamic heat accumulation of the coating/substrate system on coating quality was normally ignored. Based on the heat input by the gas flow and impacting particles, the substrate/coating system experience gradual heating process [28]. Such dynamic heat accumulation is mainly affected by the nozzle trajectory manipulated by the industrial robot. Thus, the temperature increase of the coating/substrate system can be affected by the nozzle movement and its trajectory according to the fabrication size of the cold sprayed coating. While accounting the substrate size's effect on thermal distribution, the academic CS studies in laboratory have a significant variation by comparing with the large-size industrial production.

Based on the previous study [29], it is found that the kinematic parameters concerning the nozzle movement such as the traverse speed and trajectory can significantly affect the coating surface temperature and further the coating quality. Therefore, the aim of this work is to investigate the influence of fabrication size and nozzle trajectory on the dynamic heat accumulation in CS and coating properties. Two types of Ni

coatings with different fabrication dimensions were deposited onto substrates via CS. The evolution of microstructure and porosity were studied in different deposition cases. Meanwhile, the mechanical properties of the cold sprayed Ni coatings were investigated, including the microhardness and tribological performance. This work aims to study the influence of substrate size and nozzle trajectory on the coating quality of cold spraying additive manufacturing, which can give the guidance to the nozzle trajectory optimization and deposition strategy improvement.

2. Experimental details

In order to evaluate the influence of dynamic heat accumulation in the CS process, cold sprayed coatings were deposited onto substrates with distinct size difference. Two types of building dimensions were used in the work to deposit CS coating on different substrates. It is able to emphasize the heat exchange between gas jet and substrate and the role of heat accumulation in the coating deposition. As shown in Fig. 1, the building dimensions of the cold sprayed coating were given as following: type I 4×7 cm, type II 10×25 cm. Coatings were fabricated by using a CGT-3000 system (LERMPS, UTBM, France). Compressed air was used as the driving gas with the pressure and the temperature at the inlet of 2.4 MPa and 360 °C, respectively. The moderate deposition parameters were used here to emphasize the role of substrate building dimension during CS process, rather than other parameters. The standoff distance between the nozzle exit to the substrate surface was 30 mm. The nozzle traverse speed was defined as 150 mm/s. Under such conditions, the coating was obtained by repeating the nozzle trajectory for 5 times. As shown in Fig. 2, the gas-atomized pure Ni powder (Praxair Surface Technologies, Inc., U.S.A) with spherical morphology was chosen as the feedstock. Aluminum (Al), copper (Cu) and stainless steel (SS) were chosen as the substrates. The powder morphology by scanning electron microscopy (SEM) as well as its size distribution are shown in Fig. 2.

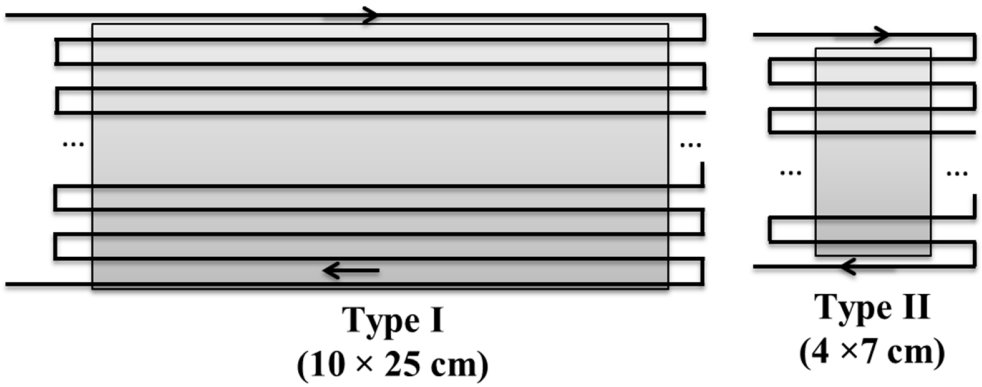

Fig. 1 Schematic diagram of the nozzle trajectory used for the deposition of cold sprayed coating.

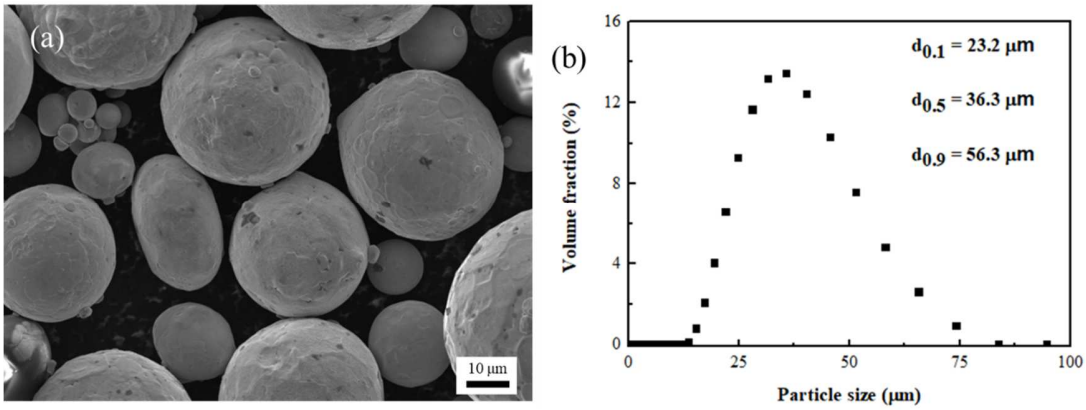

Fig. 2 (a) SEM morphology and (b) size distribution of Ni particles used in this work.

Microstructure of the cold sprayed coating was examined by optical microscope (OM, Nikon, Japan). The average porosity value of deposited coating was evaluated by image analysis software (ImageJ, NIH, Bethesda, Md.) based on ten images. In order to evaluate the temperature evolution during the coating build-up process, the temperature history of coating surface was measured and simultaneously recorded by a thermal imaging camera (SC5000, FLIR Systems, U.S.A). The temperature variation at the middle point of coating surface was continuously recorded by the measurement software. The camera operating at a frequency of 10 Hz and a waveband of 2.5-5.1 μm was fixed on a tripod with about 1.0 m away from the sample.

The Vickers hardness was measured at the cross-sectional areas of polished samples using a microhardness tester (Leiz-Wetzlar, Germany) at a load of 300 g and an indentation time of 25 s. The microhardness result is the average of 15 measurements. Dry sliding wear tests were conducted at ambient

temperature with a CSEM tribometer implement (Switzerland). Before the tests, the roughness *Ra* of the sample was polished less than 0.15 μm to rule out its influence. The counterpart material was a WC/Co ball with a diameter of 6 mm, which was polished and cleaned with ethanol before the tests. The friction test load was 500 g, with a rotational speed corresponding to 100 mm/s for 100 m with the radius of 3 mm. The coefficient of friction (COF) was recorded during sliding. After friction test, the surface of worn samples was observed by a scanning electron microscope (SEM) (JSM5800LV, JEOL, Japan). The cross-sections of the worn tracks were measured by an Altisurf 500 profilometer (France). The worn volumes of the samples were calculated via the product between the cross-sectional areas and length of worn tracks. To evaluate the wear resistance performance, the wear rate of friction test is defined as the worn volume per unit of normal load and sliding distance, where the formula is given as following [30]:

$$\omega = \frac{2\pi r S}{pl},$$

where ω is the wear rate in $mm^3/(N \cdot m)$, r is the wear radius in mm, S is the cross-sectional area in mm^2, p is the normal load in N, l is the sliding distance in m.

3. Experimental results

3.1. Coating microstructure

Fig. 3 shows the distinct microstructures of Ni coatings with different building dimensions. The dense Ni coatings of type II can be clearly seen with no obvious pores. On the contrary, the higher porosity level exists in the type I coatings deposited on substrate at three different material types. As the magnified view is given in Fig. 4, the type I coatings present inter-particle cracks and pores at all three substrate materials. However, as for type II, the Ni coatings are fully dense without such cracks or pores. As it is given in Fig. 5, the porosity values of type II coatings are well remained below 0.5%. At three different substrate materials, the interior defects like pore and cracks are more prominent in the cases of type I coatings, and the highest value of about 5% was obtained at SS substrate.

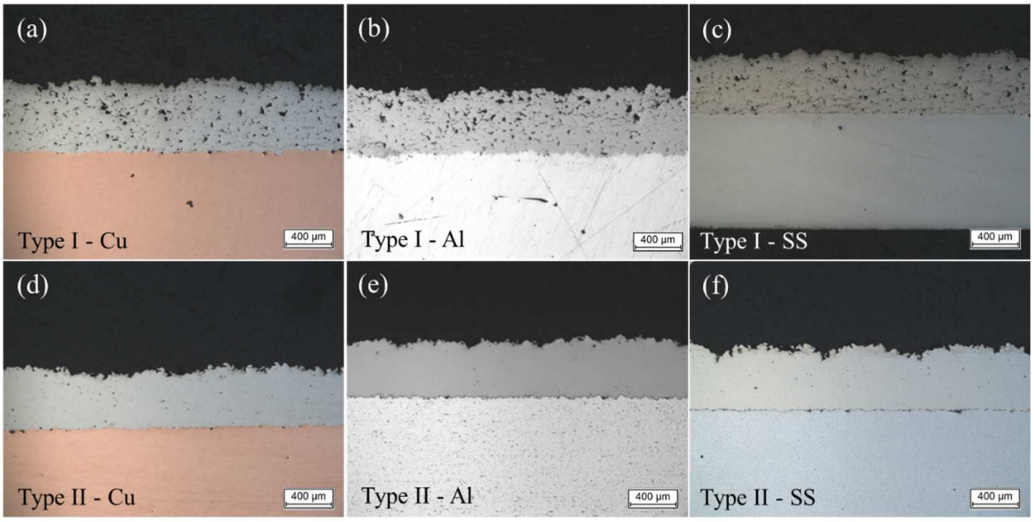

Fig. 3 Microstructure of the Ni coatings with different building dimensions: (a-c) type I, (d-f) type II.

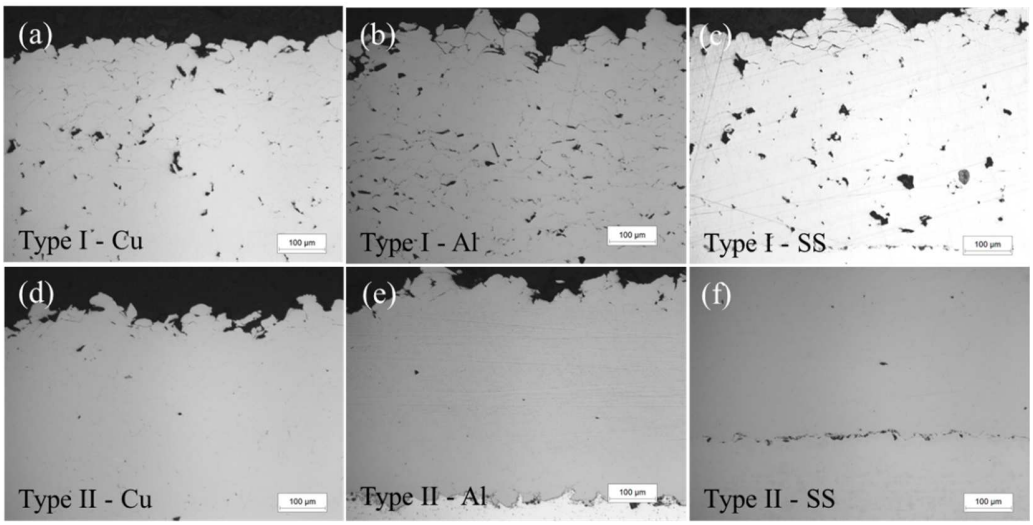

Fig. 4 Magnified views of the coating microstructure with different building dimensions: (a-c) type I, (d-f) type II.

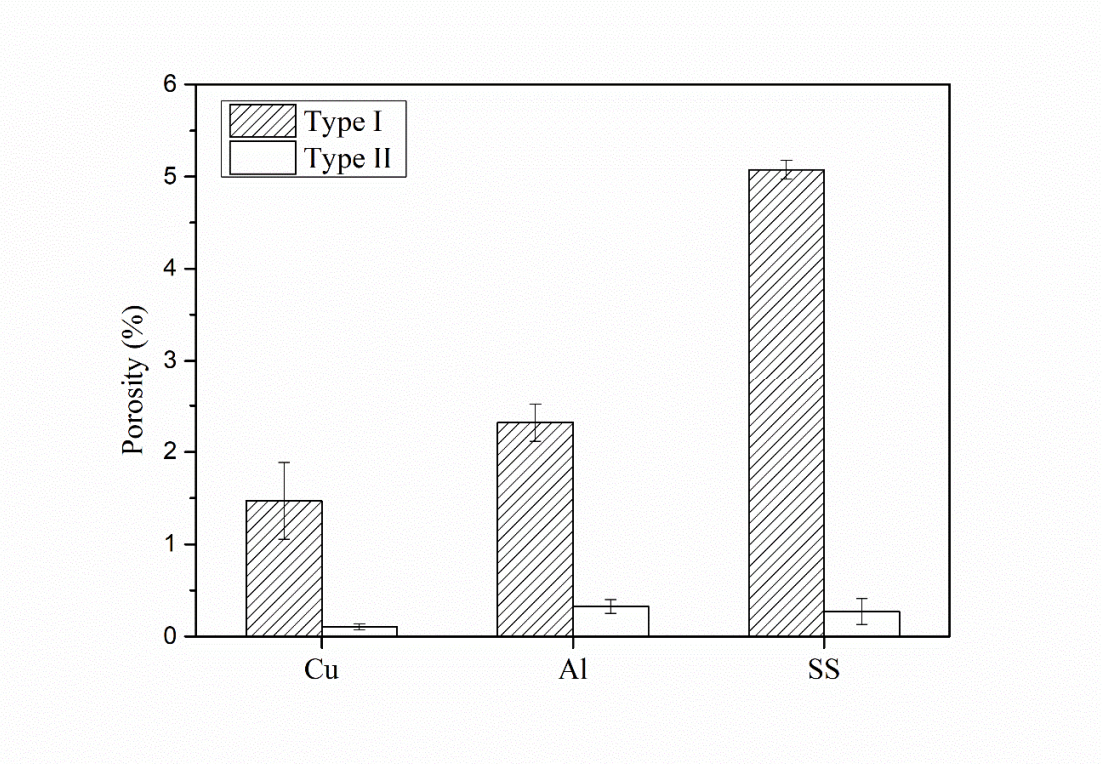

Fig. 5 Porosity of the Ni coatings at different substrates with various materials.

3.2. Microhardness

Fig. 6 illustrates the microhardness variation of Ni coatings at different building dimensions. It can be seen that the type II coatings with different material types possess a similar microhardness value around 400 $HV_{0.3}$. However, the type I coatings present a relatively lower microhardness value by comparing with the type II samples. Meanwhile, it is worth noticing that the type I coating deposited on the SS substrate has the lowest microhardness due to the highest porosity level.

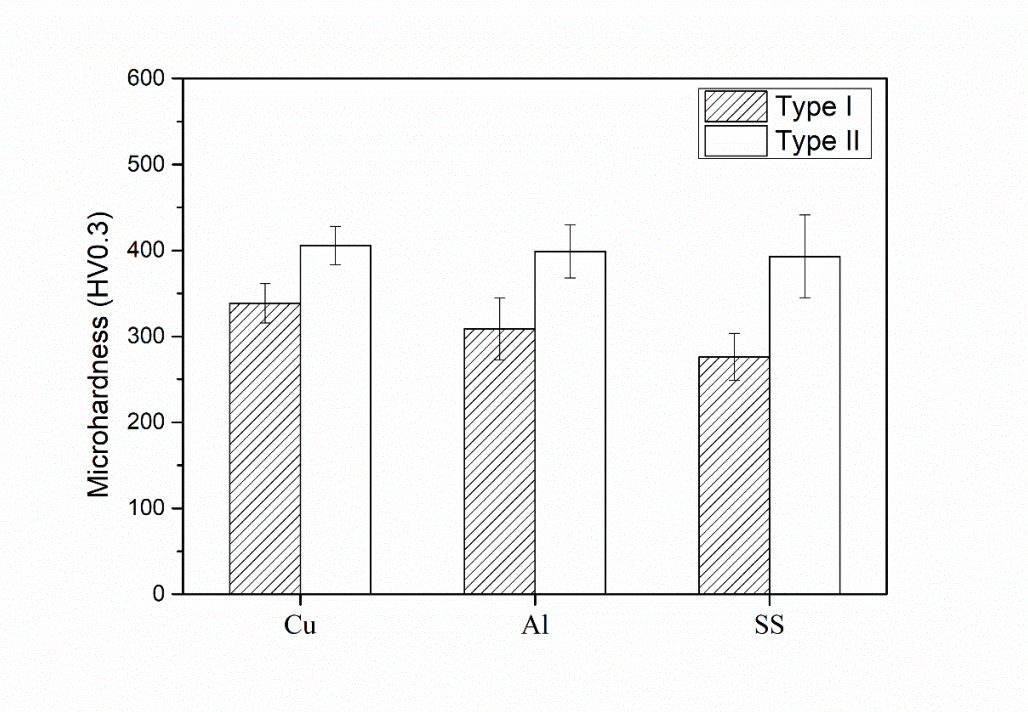

Fig. 6 Variation of microhardness of the Ni coating on different deposition conditions.

3.3. Wear performance

The wear rates of Ni coatings deposited at different conditions were shown in Fig. 7. It is obvious that the type I coatings possess higher wear rates than the ones of the type II. The variation of wear rates in tribological test has a similar trend with the microhardness values (see Fig. 6). Table 1 shows the variation of coefficients of friction (COF) at different coating deposition conditions. It is evident that the type II coatings present a relatively lower COF value than those of type I. As reported by Alidokht et al. [30] on the dry-sliding test of cold sprayed pure Ni coatings, the coating with a porosity value of 3.8% showed comparable wear rate values. It indicates a good wear-resistance performance was obtained for the type II Ni coatings.

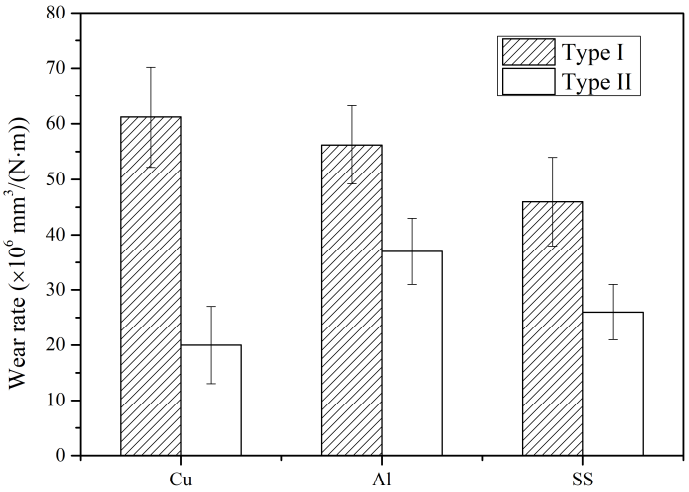

Fig. 7 Wear rate of the Ni coatings deposited at different conditions.

Table 1 Experimentally measured coating coefficients of friction (COF).

	Ni/Al	Ni/Cu	Ni/SS
Type I	0.526 ± 0.027	0. 516 ± 0.017	0. 526 ± 0.015
Type II	0.471 ± 0.034	0. 509 ± 0.034	0. 508 ± 0.015

To further understand the wear-resistance of the cold sprayed Ni coating deposited at different conditions, the worn morphologies were given in Fig. 9. All the worn surfaces show the existence of evident tribolayer with different morphologies. As for the cold sprayed Ni coatings, such tribolayer can be easily formed due to the existence of refined grain following dynamic recrystallization. These grain boundaries can further induce the formation of oxide tribolayer through the mechanical mixing and smearing of wear debris during sliding [31]. Generally, such tribolayer can benefit the wear resistance of the coating surface by lowering the friction coefficient and protecting the interior coating from further sliding of the counterpart. The formation of tribolayer on worn surface contributes to a third-body abrasion in the sliding process and gives rise to heterogeneous deformations, which could significantly decrease the COF value and prevent serious ploughing of the worn tracks. However, distinct surface morphologies can be noticed on the worn tracks of Ni coatings deposited at different conditions. From the overview observation (see Fig. 9 (a), Fig. 8 (a) and Fig. 10 (a)), large-size delamination can be seen on the worn track surface of the type I Ni coatings. As for the type II coatings, cracks are visible on the worn surface without

signs of large delamination exposing the interior Ni coatings. It is known that this kind of tribolayer formed during sliding test tends to have low toughness and easily to form such micro-sized cracks. Under the successive contact loading by the counterpart, the maximum shear stress will be initiated inside the tribolayer, which can cause the plastic shear deformation on worn surface. Afterwards, the low-cycle surface fatigue can be induced under the successive loading by counterpart [32], whereas the cracks are initiated while exceeding the yield strength of Ni phase. With the further sliding, these cracks will be propagated along the direction of maximum shear stress across the formed tribolayer. Finally, the observed delamination on the tribolayer will be formed and leads to the exposure of interior coating [31].

Thus, it can be convinced that the wearing mechanism of the type I coatings can be characterized by the localized delamination of the tribolayer on the worn surface under the cyclic fatigue of the sliding. With the continuous peeling of the cracked tribolayer, the unprotected Ni coating is exposed under friction of counterpart, which can lead to an unstable variation of COF and a higher wear rate in the cases of type I coatings. In addition, the adhesion wear and delamination of tribolayer are significantly weakened in the type I Ni coatings. Such difference in wear mechanism and wear-resistance can be contributed to the increased microhardness and densified coating morphology for the Ni coatings of type II.

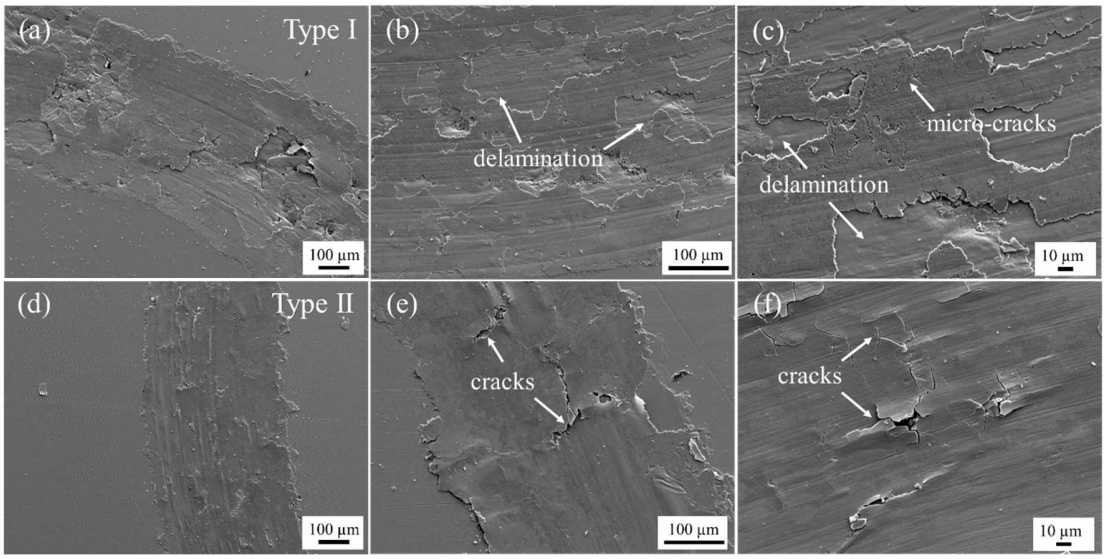

Fig. 8 Worn morphologies of Ni coatings on Cu substrates with different magnifications: (a-c) type I, (d-f) type II.

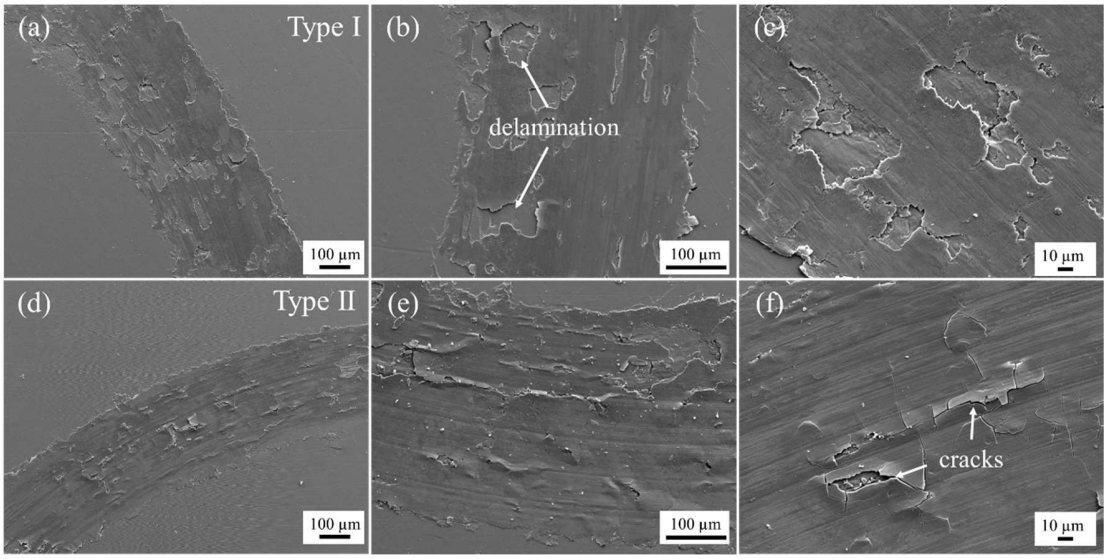

Fig. 9 Worn morphologies of Ni coatings on Al substrates with different magnifications: (a-c) type I, (d-f) type II.

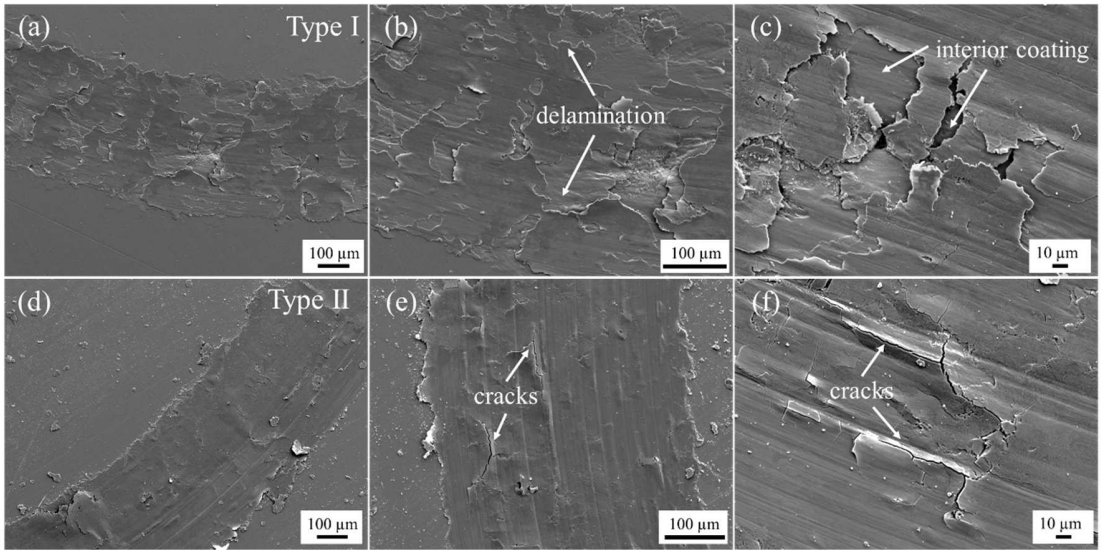

Fig. 10 Worn morphologies of Ni coatings on SS substrates with different magnifications: (a-c) type I, (d-f) type II.

4. Discussion

Generally, the cold sprayed coating is formed based on the process of layer-by-layer deposition. After the deposition of the first layer on substrate, the successive impacts of subsequent particles onto the already formed coating layer lead to the progressive coating formation process. However, to the author's knowledge, most efforts were made on the substrate preheating prior to deposition by the CS community [24, 25]. The dynamic heat accumulation during the deposition process is usually neglected in most studies.

In this work, the heat accumulation of coating/substrate system is controlled through a well-designed experiment. It is found that the coating quality, microstructure features and mechanical properties can be directly controlled by the coating temperature during deposition process.

In order to further understand the microstructure evolution of the Ni coatings with different building dimensions, the temperature evolution of the coating/substrate surface was recorded by thermal imaging camera. A thermal imaging example of the Ni coating deposition on Al substrates with different sizes is given in Fig. 11. With the color indicating temperature values according to the legend, the type II sample shows a significantly higher surface temperature than the one of type I. As the temperature histories of all cases are given in the Fig. 12, it is obvious that all the type I coatings with different substrate materials possess a relatively lower temperature compared with the ones of type II. Fig. 13 gives the average temperature on coating surface at different conditions. It is obvious that the type II coatings possess a higher surface temperature than that of type I. The nozzle trajectories of type I coatings lead to a lower surface temperature due to the longer cooling duration following the impinging of gas flow. Besides, the thermal properties of the substrate can also have a direct influence on the surface temperature of coating/substrate system, especially the thermal conductivity (k). As shown in Fig. 13, lower surface temperature values were obtained for the coatings deposited on substrates with higher thermal conductivity values. The Ni coating on the Cu substrate with a k value of 386 W/(m*K) possessed the lowest surface temperature. Such decreased surface temperature is due to the enhanced heat dissipation between the coating and the substrate at a higher thermal conductivity value.

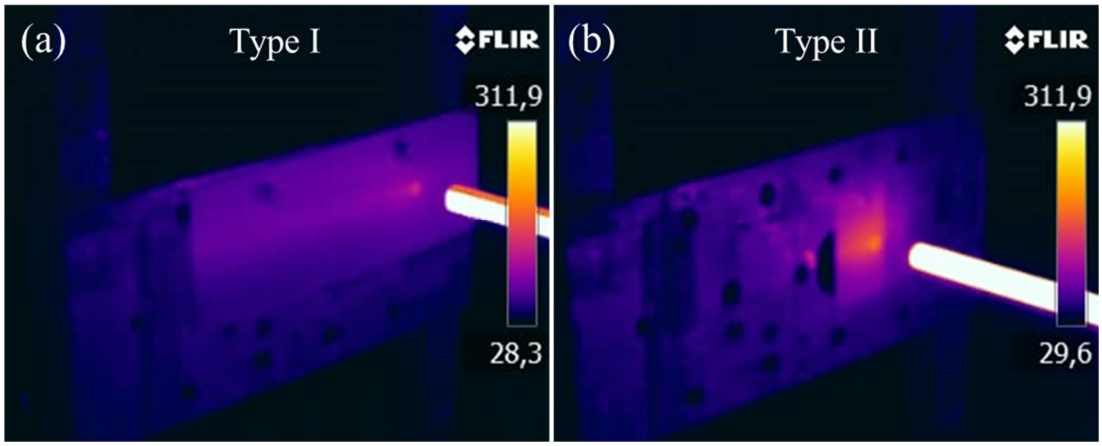

Fig. 11 Thermal imaging of the deposition process of cold sprayed Ni coating on Al substrates with different sizes: (a) type I and (b) type II.

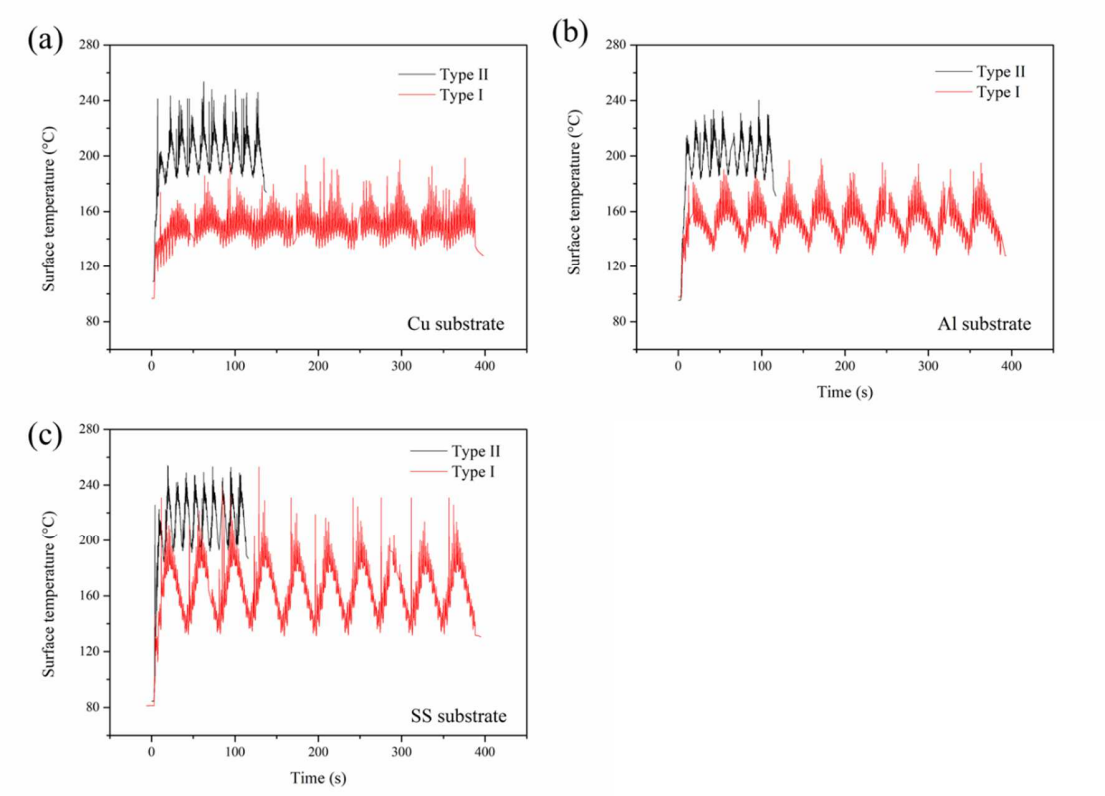

Fig. 12 Temperature history of the coating/substrate surface recorded by thermal imaging camera for different substrate types: (a) Cu, (b) Al and (c) SS.

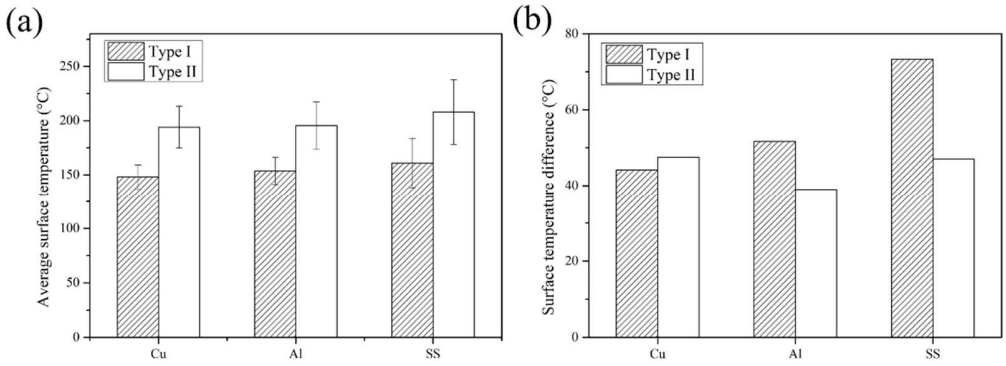

Fig. 13 (a) Average surface temperature and (b) surface temperature difference of the Ni coating on different deposition conditions.

In the cases of type I coatings, the Ni particles were deposited onto the already formed coating layers with lower temperature due to longer traverse distance. Thus, the resulting weakened particle deformation at lower thermal softening effect can provide less chances for the formation of strong mechanical

interlocking. It can be explained by the existing defects like pores and cracks as well as a higher porosity value. On the contrary, the type II Ni coatings were indirectly preheated due to the shorted nozzle trajectory and weakened cooling. Upon the impact of successive particles, the already formed coating layers with higher temperature values highlight increasingly intensive plastic deformation. It can promote the formation of mechanical interlocking of deposited particles and eliminate the formed defects in the coatings. At the same time, the enhanced plastic deformation can also assist the breaking and cleaning of native oxide film on particle surface [33]. The exposure of fresh metal can result in the formation of metallurgical bonding and a higher cohesive strength within coating. Thus, the dense microstructure with significantly decreased porosity value were obtained in type II coatings. Such phenomena can be comparative with the studies on substrate preheating in CS. It was widely reported that the substrate preheating prior to coating deposition can effectively eliminate the coating defects and improve the adhesive strength [24, 25].

Similarly, the type II coatings possess higher microhardness values than that of type I (see Fig. 6). As it was reported in related works, the microhardness of cold sprayed coatings can be weakened by the means of particle or substrate preheating [27]. It is mainly due to the enhanced thermal softening effect that can weaken the work-hardening effect formed during particle plastic deformation. However, due to the limited temperature difference between both building dimensions, the increased microhardness is mainly attributed to the enhanced density and eliminated pore-like defects. The promoted plastic deformation of deposited particle and the already-formed coating layer can have an increased work-hardening effect than that by thermal softening.

Besides, the tribological tests show that the Ni coatings present a significantly improved wear-resistance in the cases of type II coatings, which all show lower COF values and decreased wear rates. Due to the densified coating microstructure, the improved microhardness value can significantly improve the wear resistance of type II Ni coatings. Thus, no serious delamination nor peeling off were observed on the worn track of type II coatings which leads to the significantly reduced wear rate values in this case. Meanwhile, the tribolayer on the worn tracks of different samples show different features. Under the cyclic loading of counterparts in sliding friction, the micro-cracks were initiated on the tribolayer due to the exceeding of strength limits. Owing to the porous microstructure of type I coatings, the formed crack

defects will be propagated from the pore defect and the resultant delamination can be seen on the worn track.

According to the discussions above, the distinct heat accumulation during the CS deposition onto different substrates can produce coatings with different properties. The enhanced heat accumulation in type II coating can results in a higher surface temperature. It can improve the plastic deformation of successive impacting particles onto the previous-deposited coating layer. The experimental results in this work may provide a potential guidance of the deposition strategy in CS additive manufacturing of large-scale component. Similar with other additive manufacturing techniques [34], the manufacturing trajectory and strategy can be the potential method to improve the uniform distribution of coating temperature, which can further decrease the stress concentration and distortion within the coating. The well-designed nozzle trajectory and deposition strategy can optimize the thermal distribution on the coating/substrate surface, and further improve the coating quality. It can also improv the production efficiency. The corresponding discussion was added in the manuscript.

5. Conclusion

In this work, cold sprayed Ni coatings were deposited on the substrates with different building dimensions to study the influence of heat accumulation on coating quality. The temperature history was recorded using an infrared imaging camera. The microstructure evolution, microhardness and tribological performance were investigated to understand the role of heat accumulation during CS deposition.

(1) According to the temperature history recorded by infrared imaging camera, lower average temperature was found at type I coating with larger size due to different heat accumulation of coating/substrate system. As for the type II coatings, the local heat accumulation of the coating/substrate owing to the short nozzle movement can result in a higher surface temperature.

(2) The results show that the type II Ni coatings possessed a fully dense microstructure without cracks, while the type I samples show a significantly higher porosity value. The increased particle plastic deformation at higher temperature of coating/substrate system can further promote the coating densification rate and further ameliorate the coating quality.

(3) The microhardness of type II Ni coatings is relatively higher than the ones of type I because of its dense microstructure. Due to the higher temperature of coating/substrate system, the higher microhardness

value can be obtained at type II coatings based on the crack-free microstructure over the thermal softening effect.

(4) The tribological tests shows that the type II Ni coatings presents a better wear resistance with lower coefficient of friction and lower wear rate. The distinct worn morphologies show that a lower microhardness and porous microstructure lead to numerous delamination and exposure of interior coating as a result of low-cycle fatigue failure.

(5) It can be summarized that the nozzle trajectory and deposition strategy can affect the temperature distribution and determine the coating qualities. This work can provide a potential guidance for the optimization of coating quality by cold spraying additive manufacturing.

Acknowledgements

As one of the authors, Yingchun XIE would like to acknowledge the supports of GDAS' Project of Science and Technology Development (Grants No. 2018GDASCX-0945), International Cooperation Project (Grants No. 201807010013), Natural Science Foundation of Guangdong Province (Grants No. 2018A0303130075), ZS-GDAS Technology Transfer Project (Grants No. 2017G1FC0003), High-level Leading Talent Introduction Program of GDAS (Grants No. 2016GDASRC-0204). As one of the authors, Chaoyue CHEN would like to acknowledge the supports of the Joint Funds of the National Natural Science Foundation of China (Nos. U1560202 and 51690162, 51604171), the Shanghai Municipal Science and Technology Commission Grant (No. 17JC1400602), and the National Science and Technology Major Project "Aeroengine and Gas Turbine" (2017-VII-0008-0102).

Reference

[1] T. DebRoy, H.L. Wei, J.S. Zuback, T. Mukherjee, J.W. Elmer, J.O. Milewski, A.M. Beese, A. Wilson-Heid, A. De, W. Zhang, Prog Mater Sci, 92 (2018) 112-224.

[2] D. Herzog, V. Seyda, E. Wycisk, C. Emmelmann, Acta Mater, 117 (2016) 371-392.

[3] D.D. Gu, W. Meiners, K. Wissenbach, R. Poprawe, Int Mater Rev, 57 (2013) 133-164.

[4] L.C. Zhang, H. Attar, Advanced Engineering Materials, 18 (2016) 463-475.

[5] L.E. Murr, S.M. Gaytan, D.A. Ramirez, E. Martinez, J. Hernandez, K.N. Amato, P.W. Shindo, F.R. Medina, R.B. Wicker, J. Mater. Sci. Technol., 28 (2012) 1-14.

[6] G.P. Dinda, L. Song, J. Mazumder, Metallurgical and Materials Transactions A, 39 (2008) 2914-2922.

[7] S. Yin, P. Cavaliere, B. Aldwell, R. Jenkins, H. Liao, W. Li, R. Lupoi, Addit Manuf, 21 (2018) 628-650.

[8] W. Li, K. Yang, S. Yin, X. Yang, Y. Xu, R. Lupoi, J. Mater. Sci. Technol., 34 (2017) 440-457.

[9] Y. Xie, C. Chen, M.-P. Planche, S. Deng, H. Liao, Surf Eng, (2017) 1-9.

[10] Y. Xie, S. Yin, J. Cizek, J. Cupera, E. Guo, R. Lupoi, Surf Coat Technol, 337 (2018) 447-452.

[11] J. Pattison, S. Celotto, R. Morgan, M. Bray, W. O'Neill, Int J Mach Tool Manu, 47 (2007) 627-634.

[12] S. Bagherifard, G. Roscioli, M.V. Zuccoli, M. Hadi, G. D'Elia, A.G. Demir, B. Previtali, J. Kondás, M. Guagliano, J Therm Spray Technol, 26 (2017) 1517–1526.

[13] C. Chen, S. Gojon, Y. Xie, S. Yin, C. Verdy, Z. Ren, H. Liao, S. Deng, Surf Coat Technol, 309 (2017) 719-728.

[14] M.E. Lynch, W. Gu, T. El-Wardany, A. Hsu, D. Viens, A. Nardi, M. Klecka, Virtual and Physical Prototyping, 8 (2013) 213-231.

[15] M. Grujicic, J.R. Saylor, D.E. Beasley, W.S. DeRosset, D. Helfritch, Appl Surf Sci, 219 (2003) 211-227.

[16] Y. Xie, M.-P. Planche, R. Raoelison, H. Liao, X. Suo, P. Hervé, Journal of Thermal Spray Technology, 25 (2015) 123-130.

[17] H. Assadi, F. Gartner, T. Stoltenhoff, H. Kreye, Acta Mater, 51 (2003) 4379-4394.

[18] K. Kim, M. Watanabe, S. Kuroda, Surf Coat Technol, 204 (2010) 2175-2180.

[19] C. Chen, Y. Xie, R. Huang, S. Deng, Z. Ren, H. Liao, Mater Lett, 210 (2018) 199-202.

[20] S. Yin, X. Wang, W. Li, H. Liao, H. Jie, Applied Surface Science, 259 (2012) 294-300.

[21] Y. Xie, S. Yin, C. Chen, M.-P. Planche, H. Liao, R. Lupoi, Scr Mater, 125 (2016) 1-4.

[22] C. Chen, Y. Xie, S. Yin, M.-P. Planche, S. Deng, R. Lupoi, H. Liao, Materials Letters, 173 (2016) 76-79.

[23] R.N. Raoelison, Y. Xie, T. Sapanathan, M.P. Planche, R. Kromer, S. Costil, C. Langlade, Addit Manuf, 19 (2018) 134-159.

[24] X. Suo, M. Yu, W. Li, M. Planche, H. Liao, J Therm Spray Technol, 21 (2012) 1091-1098.

[25] Y. Xie, M.-P. Planche, R. Raoelison, H. Liao, X. Suo, P. Hervé, J Therm Spray Technol, 25 (2016) 123-130.

[26] Y. Xie, M.-P. Planche, R. Raoelison, P. Hervé, X. Suo, P. He, H. Liao, Surf Coat Technol, (2016).

[27] S. Yin, X. Wang, X. Suo, H. Liao, Z. Guo, W. Li, C. Coddet, Acta Mater, 61 (2013) 5105-5118.

[28] S. Yin, M. Meyer, W. Li, H. Liao, R. Lupoi, J Therm Spray Technol, 25 (2016) 874-896.

[29] C. Chen, Y. Xie, C. Verdy, R. Huang, H. Liao, Z. Ren, S. Deng, Surf Coat Technol, 326 (2017) 355-365.

[30] S.A. Alidokht, P. Manimunda, P. Vo, S. Yue, R.R. Chromik, Surf Coat Technol, 308 (2016) 424-434.

[31] X.Y. Li, K.N. Tandon, Wear, 245 (2000) 148-161.

[32] S. Yin, E.J. Ekoi, T.L. Lupton, D.P. Dowling, R. Lupoi, Mater Des, 126 (2017) 305-313.

[33] K. Kim, S. Kuroda, Scr Mater, 63 (2010) 215-218.

[34] L. Parry, I.A. Ashcroft, R.D. Wildman, Addit Manuf, 12 (2016) 1-15.